Astron. Astrophys. 319, 839–849 (1997)

ASTRONOMY
AND
ASTROPHYSICS

Rotating globular clusters

III. Evolutionary survey

Pierre-Yves Longaretti[1] **and Christophe Lagoute**[2]

[1] Laboratoire d'Astrophysique de l'Observatoire de Grenoble, B.P. 53, F-38041 Grenoble Cedex 9, France
[2] Observatoire Midi-Pyrénées, 14 avenue E. Belin, F-31400 Toulouse, France

Received 13 May 1996 / Accepted 27 August 1996

Abstract. We describe a simple model which allows us to investigate the effects of rotation on the evolution of globular clusters and of their flattening. The model relies on a generalization to rotating clusters of sequences of quasi-equilibrium models known as King sequences, which are able to follow the evolution of globular clusters prior to core collapse. Our model includes in a simplified way the effects of internal relaxation, tidal heating by passage through the Galactic disk, and stellar evolution. We investigate a broad range of initial conditions in the cluster mass, Galactocentric distance, initial mass function power-law index, initial concentration, and initial rotation energy. We also report the results of a similar study of the Large Magellanic Cloud clusters. The major findings of this investigation are the following: i) the combined effects of rotation, tidal shocking and stellar evolution is to reduce the domain of survival of rotating clusters to higher concentrations with respect to nonrotating ones; ii) rotating clusters reach core collapse at lower concentrations than their nonrotating counterparts; iii) the three modelled processes are likely to be responsible for the luminosity/flattening and relaxation timescale/flattening correlations reported in the literature; iv) the larger flattening of the Magellanic globular clusters is mostly the result of their large spread in age, as reported by Frenk and Fall (1982), and, to a lesser extent, of the smaller efficiency of the evolution in the Magellanic Cloud tidal environment with respect to the Galaxy, assuming similar initial conditions.

Key words: celestial mechanics, stellar dynamics – globular clusters – galaxies: star clusters – Magellanic Clouds

1. Introduction

Globular clusters are often modeled as spherically symmetric systems. However, their apparent flattening can be as large as 0.7, with an average of the order of 0.9 (Frenk and Fall, 1982), and is likely produced by the cluster rotation, as the minor axis does not correlate with the direction of the Galactic center (Geyer et al. 1983; White and Shawl 1987) and as kinematic data suggest that clusters are flattened along the kinematical minor axis (Davoust 1986; Lupton et al. 1987).

Cluster flattening is observed to correlate with various quantities, such as the cluster age (Frenk and Fall 1982), half-mass relaxation time (Davoust and Prugniel 1990) and luminosity (Van den Bergh and Morbey 1984), all of which betray the influence of two-body relaxation on the evolution of cluster flattening; however, one can expect that the other processes which are known to affect sensibly globular cluster evolution, gravitational shocking and stellar mass loss, have some influence on this issue. Furthermore, the rotational energy needed to produce such flattenings, although not dominant, is nevertheless able to affect globular cluster evolution in a noticeable way (Lagoute and Longaretti, 1996, Paper I; Longaretti and Lagoute, 1996, Paper II).

The purpose of the present paper is to investigate these issues through an evolutionary survey of the Galactic clusters testing a wide range of possible initial conditions, and which takes into account (albeit in a somewhat crude way) the effects of internal relaxation, stellar mass loss and gravitational shocking on tidally truncated rotating clusters. We have also conducted a similar survey of the Large Magellanic Cloud clusters. Some results are mentioned in the conclusion of the paper.

As rotation destroys the spherical symmetry of globular clusters, direct numerical integration of the Fokker-Planck equation would be unfeasible on today's computers for the large number of initial conditions considered in this paper. On the other hand, rotation is expected to be mostly important in the initial phases of cluster evolution, prior to core collapse, and before most of the rotational energy has been carried away by escaping stars. In these phases, cluster evolution is more or less well approximated by sequences of equilibria known as King sequences (King 1966; Wiyanto et al. 1985), somewhat like the evolution of stars on the main sequence. In the two previous papers in this series, we have extended this concept to rotating clusters. This provides us with an appropriate tool for the present evo-

Send offprint requests to: P.Y. Longaretti

lutionary survey, which parallels a similar one by Chernoff and Shapiro (1987) for non rotating clusters. The strong point of this type of analysis is its simplicity, which allowed us to compute several tens of thousands of evolutionary tracks, thus gaining a broad view of the evolution, while keeping some confidence in the evolutionary trends which show up. The weak points are that the evolution is computed in a rather crude way, that we are not able to follow it through core collapse, and limited to clusters on nearly circular orbits around the parent galaxy. Thus most of the discussion of the paper focuses on general trends and a qualitative analysis of the processes at work rather than on detailed quantitative results.

Previous work on globular cluster rotation is very scant, both because rotation is not expected to influence the evolution in a dramatic way, and because the loss of spherical symmetry is a major complication. Shapiro and Marchant (1976) were interested in explaining why globular clusters were much more spherical than elliptical galaxies at a time where the flattening of these objects was thought to be produced by rotation. They modelled globular clusters as incompressible ellipsoids, and used the old relaxation argument by Ambartsumian (1938), and Spitzer (1940), as formulated by Agekian (1958) for rotating systems, to compute the mass, energy and angular momentum losses due to internal relaxation and which make the model evolve in time. They concluded that globular clusters tend to become more spherical as they evolve if their initial flattening is smaller than some critical value, otherwise they become more flattened. More recently, Goodman (1983) has followed the collapse of a few rotating cluster models with a numerical integration of the Fokker-Planck equation, and found that relaxation is able to explain the loss of cluster flattening.

The paper is organized as follows. Sect. 2 presents our evolutionary model. A qualitative picture of the effects of internal relaxation, stellar evolution and gravitational shocking is also developed there. Our numerical results are presented and discussed in Sect. 3. Sect. 4 summarizes the main implications for the Galactic and Magellanic Clouds globular cluster systems.

2. Evolutionary model

We represent globular clusters with a distribution function depending on two integrals of the motion (the energy E and the component of the angular momentum along the rotation axis L_z) which generalizes King's distribution to rotating clusters and reads

$$f(E, L_z) = C\left[\exp(-\beta(E - \Phi_t)) - 1\right]\exp(\beta\Omega L_z), \qquad (1)$$

if $E < \Phi_t$ and $f = 0$ otherwise. This model was chosen because it is an approximate solution of the Fokker-Planck equation in the evaporation phase (see paper II), and because it reduces to King models for nonrotating clusters. We call it a rotating King model in the remainder of the paper. We have ignored the dependence on the third integral of the motion for numerical tractability. Physically, this implies that we ignore the radial anisotropy of the velocity dispersion unavoidably produced by internal relaxation (this is further discussed in Sect. 4). The properties of this model are discussed in paper I.

This model is described by four parameters, e.g. (C, β, Φ_t, Ω) or the total mass M_t, total energy E_t, total angular momentum along the rotation axis L_t, and radius of truncation r_t. Because this model is an approximate solution of the Fokker-Planck equation, its evolution under two-body relaxation reduces to the evolution of these parameters. The other processes considered in this paper (gravitational shocking and stellar evolution) are assumed *not* to affect our basic adopted form for the distribution function, and their contribution to the evolution is also computed through their contribution to the rates of variation of the cluster total mass, energy and angular momentum. Finally, the cluster is assumed to fill its tidal radius so that the truncation radius r_t is fixed by the tidal constraint.

2.1. Tidal constraint and Galactic potential

For circular or nearly circular orbits of radius R_G around the Galaxy, the galactic tidal field limits the cluster size r_t to

$$r_t = R_G\left(\frac{M_t}{3M_G}\right)^{1/3}, \qquad (2)$$

where M_G is the mass of the Galaxy inside the globular cluster orbit. For Galactic globular clusters, tidal radii are computed from the Galactic model of Bahcall et al. (1982). This model admits nearly circular orbits with arbitrary inclination angle with respect to the Galactic disk. Equation (2) can be generalized to non-circular orbits, but this sophistication is not required here, considering the crudeness of our evolutionary model.

2.2. Two-body relaxation

In the evaporation phase, two-body relaxation drives nonrotating globular clusters to states of higher concentration until the gravothermal core collapse sets in. In the process, some stars gain energy and are lost by the cluster as they cross the tidal boundary. One generally makes the (somewhat uncorrect) assumption that stars are actually lost when they cross the energy boundary Φ_t in energy space. Furthermore, the cluster loses the mass and energy carried away by these escaping stars.

This is also true for rotating clusters. The Fokker-Planck collision term evaluated at the cluster energy boundary allows us to compute the loss rates of mass, energy and angular momentum of the cluster which are needed in our evolution scheme. The computation is detailed in paper II, and the relevant expressions reproduced in the appendix.

2.3. Gravitational shocking

When a cluster crosses the galactic plane, the work done by the tidal force of the disk on the cluster stars heats the cluster, and also causes it to lose some of its less bounded stars. This effect was first analyzed by Ostriker et al. (1972) and Spitzer and Chevalier (1973) in the impulse approximation. Chernoff et al.

(1986) have refined this initial analysis. In particular they included an adiabatic cut-off in the response of the more bounded stars to the disk force, as these stars can have orbital times comparable to or shorter than the characteristic time of cluster transit through the Galactic plane, and they considered the contribution of the shock-induced mass loss to the heating of the cluster. More recently, Weinberg (1994a,b and c) has shown that the harmonic model of Chernoff et al. (1986) produces an unrealistic exponential adiabatic cutoff (instead of a power-law), resulting in an underestimation of the efficiency of gravitational shocking by about a factor of two.

In the present work, we have taken advantage of the fact that rotation produces only perturbations to the structure of a cluster for realistic cluster flattening, so that one expects the mass and energy loss induced by gravitational shocking on our rotating models to be reasonably well approximated by the losses of the equivalent nonrotating King model. These King model losses have been studied in detail by Chernoff et al. (1986). The changes in the cluster total mass and energy produced by gravitational shocking can be parameterized by (Chernoff and Shapiro 1987):

$$\left(\frac{dM_t}{dt}\right)_{\rm sh.} = -2f_p\left(\frac{GM_t}{r_t}\right)^{-1}\Delta T_t\,, \tag{3}$$

$$\left(\frac{dE_t}{dt}\right)_{\rm sh.} = 3f_p\Delta T_t\,, \tag{4}$$

where f_p is the frequency of passage through the Galactic plane, and ΔT_t is the change in kinetic energy of the cluster produced in a single passage:

$$\Delta T_t = 2.56\times10^3\left(\frac{M_t}{10^5 M_\odot}\right)^{5/3}\times \left[\frac{s(W_0)}{s(1)}\right]\mathcal{Q}(R_G,\theta,W_0)\,M_\odot{\rm km}^2{\rm s}^{-2}\,. \tag{5}$$

In Eq. (5), $s(W_0)$ is the mean square radius of a King model of dimensionless central potential W_0 (see the appendix), θ is the angle with which the globular clusters passes through the disk, and $\mathcal{Q}(R_G,\theta,W_0)$ a function tabulated by Chernoff et al. (1986). In practice, the efficiency of tidal heating depends little on θ unless the cluster orbits very close to the Galactic plane; for definiteness, we have chosen $\theta=\pi/4$.

To estimate the change of angular momentum, we first note that gravitational shocking produces no change in the total cluster angular momentum on non escaping stars, either in the impulse approximation or with the simple harmonic stellar motion prescription of Chernoff et al. (1986). Also, escaping stars have a mean radius $\sim 0.6r_t$ (Chernoff et al. 1986). For these radii, our cluster model typically yields $\langle L_z\rangle \lesssim m_{\rm star}L_t/M_t$. As our evolutionary model is rather crude in any case, we are therefore motivated to take

$$\left(\frac{dL_t}{dt}\right)_{\rm sh.} = \frac{L_t}{M_t}\left(\frac{dM_t}{dt}\right)_{\rm sh.}\,. \tag{6}$$

To conclude, we stress that gravitational shoking tends to depopulate the halo of globular clusters. If the halo is not replenished fast enough through relaxation in the cluster center, our assumption that the tidal radius is filled or of a rotating King model for the cluster might be invalidated during the evolution.

2.4. Stellar evolution

Stellar mass loss occuring during stellar evolution provides an important source of globular cluster heating, especially during the first billion years of the cluster lifetime, as heavy stars evolve much faster on the main sequence and provide the largest contribution to the mass loss. In principle, a multimass cluster model is required to account for this phenomenon with some accuracy, especially since these models evolve faster by internal relaxation than any single mass model whose mass is chosen in the mass range of the multimass model, due to the faster energy conduction between different mass components with respect to energy diffusion in a single component (Inagaki 1985; Chernoff and Weinberg 1990). Therefore, the relaxation model described above is strictly designed for a single mass model, and the simple approximation used below to account for an initially wide stellar mass spectrum can only represent the heating phenomenon in a rather crude way.

Following Chernoff and Weinberg (1990), we assume an initial mass function $F(m)\propto m^{-\alpha}$ for $0.35\ {\rm M}_\odot < m < 14\ {\rm M}_\odot$. The mass function is defined such that $M_t=\int F(m)\,dm$. The lifetime on the main sequence is $t_{\rm m.s.}\simeq(1\ {\rm M}_\odot/m)^3\times10^{10}$ yrs, and the stars are assumed to shed instantaneously a mass δm at the end of their main sequence lifetime. This mass loss δm is taken from Miller and Scalo (1979), i.e., $\delta m = 0.78m - 0.36$ if $m < 4.7\ {\rm M}_\odot$, $\delta m = m$ if $4.7\ {\rm M}_\odot < m < 8.0\ {\rm M}_\odot$ and $\delta m = m - 1.4$ if $m > 8.0\ {\rm M}_\odot$.

With this model, mass loss is essentially efficient in the initial phases of globular cluster evolution, as generally more than two-thirds of the total stellar mass loss occur in the first few giga-years of the cluster evolution, for the values of α considered in this paper. Recent observational and modalisation work has shown that the mass function is likely to reach lower mass limits than the one assumed here to conform with past usage (see, e.g., Piotto 1995; Gebhardt and Fisher, 1995; Taillet et al. 1996), but this will not affect in any way the results presented here, as the main sequence lifetime of these low mass stars is extremely long.

For an idealized homogeneous model, the mass, energy and angular momentum losses per unit time read

$$\left(\frac{dM_t}{dt}\right)_{\rm stel.} = \frac{F(m)\delta m}{m}\left(\frac{dt_{\rm m.s.}}{dm}\right)^{-1}\,, \tag{7}$$

$$\left(\frac{dE_t}{dt}\right)_{\rm stel.} = 3\frac{E_t}{M_t}\left(\frac{dM_t}{dt}\right)_{\rm stel.}\,, \tag{8}$$

$$\left(\frac{dL_t}{dt}\right)_{\rm stel.} = \frac{L_t}{M_t}\left(\frac{dM_t}{dt}\right)_{\rm stel.}\,. \tag{9}$$

Two-body relaxation induces a mass segregation in the cluster. As a consequence, these simple estimates tend to underestimate the disruption of clusters by stellar mass loss, but maximize the loss of angular momentum.

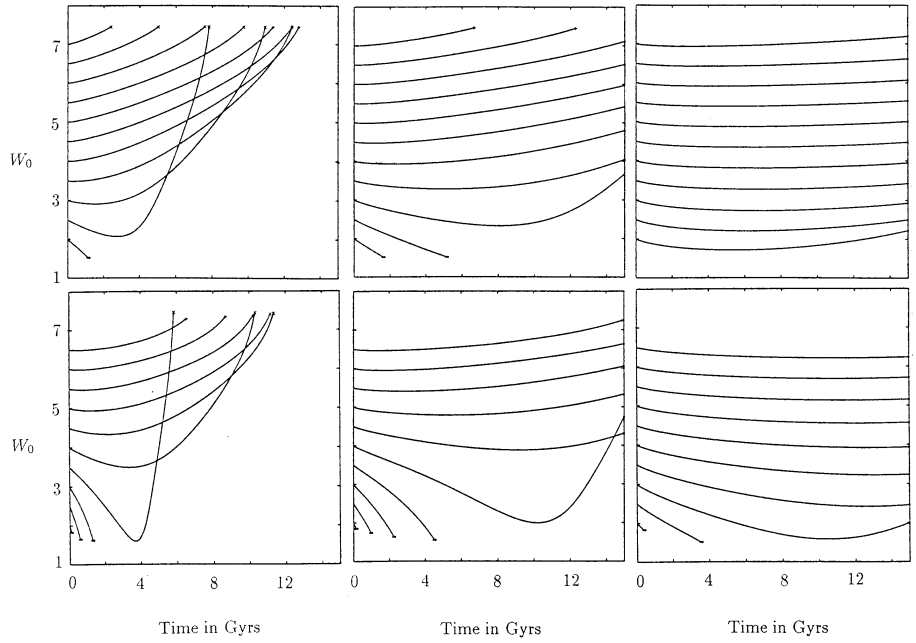

Fig. 1. Evolution of the concentration as a function of time in Gyrs for 10^5 $M_\odot$ clusters initially, and for α = 3.5. Upper-half: nonrotating clusters; lower-half: clusters with 15% of rotation energy. Diagrams from left to right correspond to Galactocentric distances of 3, 8 and 14 kpcs respectively. Clusters reaching $W_0 \sim 1.5$ are assumed to dissolve, while those reaching $W_0 \sim 7.4$ are assumed to collapse (see Sect. 3.1 for details).

2.5. Qualitative description of the evolution

The evolution of two of the dimensionless parameters of interest here, the cluster central dimensionless potential W_0, which is a monotonic function of the cluster concentration (even for rotating models), and the cluster flattening, can be constrained from the general knowledge of the rates of variation of the cluster global quantities (M_t, E_t, and E_T) described above. Let us define a dimensionless total energy (King 1966) and angular momentum by

$$\nu = \frac{E_t}{(GM_t^2/r_t)}, \tag{10}$$

$$\lambda = \frac{L_t|E_t|^{1/2}}{GM_t^{5/2}}. \tag{11}$$

The time variation of these quantities can be directly obtained from the equations presented above. It is also useful to relate the energy and angular momentum loss rates to the mass loss rates by two dimensionless parameters, f and g, defined by

$$\frac{1}{E_t}\frac{dE_t}{dt} \equiv -\frac{f}{\nu M_t}\frac{dM_t}{dt}, \tag{12}$$

$$\frac{1}{L_t}\frac{dL_t}{dt} \equiv \frac{g}{M_t}\frac{dM_t}{dt}. \tag{13}$$

From these definitions, we obtain for the evolution of ν and λ

$$\frac{1}{\nu}\frac{d\nu}{dt} = -\left(\frac{f}{\nu}+\frac{5}{3}\right)\frac{1}{M_t}\frac{dM_t}{dt}, \tag{14}$$

$$\frac{1}{\lambda}\frac{d\lambda}{dt} = \left(g-\frac{f}{2\nu}-\frac{5}{2}\right)\frac{1}{M_t}\frac{dM_t}{dt}. \tag{15}$$

In first approximation, ν depends mostly on the cluster concentration and is a decreasing function of W_0, while λ depends mostly on, and is an increasing function of, the cluster flattening (see Figs. 9a&b of paper II). Therefore, as a rule of thumb, one can assume that the cluster concentration increases when $\nu < -3f/5$ and its flattening decreases when $g < f/2\nu + 5/2$. For two-body relaxation, f = 1 and $g \gtrsim 2$ (see paper II) which indicates that a cluster concentration always increases while its flattening decreases by internal relaxation. Gravitational shocking is characterized by $f = 3/2$ and $g \lesssim 1$; this produces an increase in cluster concentration if $W_0 \gtrsim 4$ and a systematic *increase* of the cluster flattening. Finally, for stellar evolution mass loss and heating we have $f = -3\nu$ which always tends to dissolve clusters, while again $g \lesssim 1$ and the flattening always tends to *increase*. These expectations based on the simple rule of thumb presented above are born out in the more detailed evolutionary calculations presented next.

3. Numerical results

The total mass M_t, total energy E_t, total angular momentum L_t and tidal radius r_t unambiguously define a cluster model, whose evolution under two-body relaxation, gravitational shocking and stellar evolution is constrained by Eqs. (A12) through (A14), (3) through (9), and (2). We have computed a large number of evolutionary tracks whose initial conditions are specified by the cluster mass M_t, dimensionless central potential W_0 (i.e. the cluster concentration), Galactocentric distance R_G, and rotation energy $T_{\rm rot}/T_t$ (T_t is the cluster total kinetic energy), which define the initial cluster model. Stellar evolution is specified by the initial spectral index of the mass function α with the additional assumption that all stars begin their main-sequence lifetime when the evolutionary track is started.

The calculation is carried out for a Hubble time t_H at most ($t_H = 1.5 \times 10^{10}$ yrs), but is stopped earlier if one of the following conditions is met during the evolution.

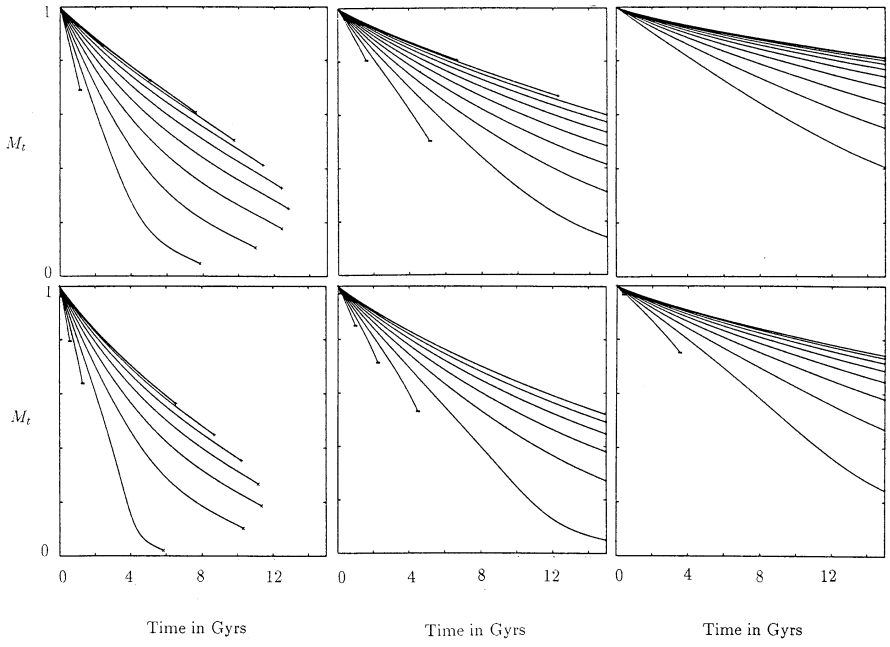

Fig. 2. Evolution of the mass as a function of time in Gyrs for clusters of 10^5 $M_\odot$ initially, and for α = 3.5. Upper-half: nonrotating clusters; lower-half: clusters with 15% of rotation energy. Diagrams from left to right correspond to Galactocentric distances of 3, 8 and 14 kpcs respectively. The various tracks correspond to initial values of W_0 ranging from 2 to 7 from bottom to top in each diagram (see Sect. 3.1 for details).

The cluster can reach the limit of thermodynamical stability. For nonrotating clusters, this happens when the concentration becomes larger than $W_{0c} \simeq 7.4$ (Katz, 1980). For our rotating cluster model, we have used the limits computed in paper I, where Katz's result is generalized to rotating clusters. Once the gravothermal instability sets in, nonrotating clusters complete core collapse in about 330 central relaxation times (Cohn, 1980). The numerical simulations of Goodman (1983) suggest that, in first approximation, this holds also for rotating clusters. Furthermore, core collapse should be relatively insensitive to gravitational shocking (which affects mostly the cluster halo) and to stellar evolution if it does not occur in the first few billion years of its evolution. Therefore, when a cluster reaches its thermodynamical stability limit, we use Cohn's result to estimate whether it is collapsed or still collapsing within a Hubble time. On the contrary, if the concentration W_0 becomes smaller than about 1.5, the integration is also stopped and the cluster assumed to dissolve. This lower limit on W_0 is imposed by the way we handle the cluster structure in our computation of its total mass, energy and angular momentum, so that it is conceivable that not all clusters reaching this limit will actually dissolve in a Hubble time; however, the evolutionary survey of Chernoff and Shapiro (1987) implies that most nonrotating clusters reaching W_0 = 1.5 will in fact also reach W_0 = 0, which provides some support to the assumption made here.

Finally, the cluster can become dynamically unstable. As in our two previous papers, we assume that this happens when the rotation energy in the cluster $T_{\rm rot}/T_t$ exceeds 28% (Ostriker and Peebles, 1974). However, this happened in our simulation only when the initial rotation energy was rather large ($> 20\%$), and is not seen in any of the evolutionary calculations reported here.

3.1. Evolutionary tracks

A sample of our evolutionary tracks is presented on Figs. 1 to 3. The initial conditions are M_t = 10^5 $M_\odot$ and α = 3.5 for all the tracks. Fig. 1 presents the evolution of the concentration, while the evolution of the (normalized) mass is shown on Fig. 2. On both figures, the upper three diagrams pertain to nonrotating clusters, and the lower three to clusters having 15% of rotation energy $T_{\rm rot.}/T_t$. Different values of the rotation energy have been explored, but the results can simply be extrapolated from the ones presented here.

Our choice is motivated by the typical rotational energy expected in ω Centauri, the most flattened cluster of the Galaxy, but also the most massive and therefore the one most likely to resemble today its initial state; a guess based on the rotational energy of the Magellanic Cloud young clusters would be preferable, but we lack the required observational data, although similar or even higher initial values of the rotational energy seem quite plausible.

In each figure, the diagrams correspond, from left to right, to Galactocentric distances of 3, 8 and 14 kpcs, respectively. Each diagram generally contains eleven evolutionary tracks, which correspond to initial values of W_0 ranging from 2 to 7 by steps of 0.5 (from bottom to top in Fig. 2, and top to bottom in Fig. 3).

Let us first comment the diagrams obtained for nonrotating clusters, before discussing the influence of rotation on the evolution (for a more detailed discussion, see Chernoff and Shapiro 1987). We merely note on Fig. 1 that, as expected, both gravitational shocking and internal relaxation are less efficient as one goes away from the Galactic center, because passages through the Galactic disc are less frequent, and the tidal truncation of the cluster less efficient. As a consequence, the timescales for collapse or dissolution become longer, while close to the Galactic center, the evolution timescales are so short that 10^5 $M_\odot$

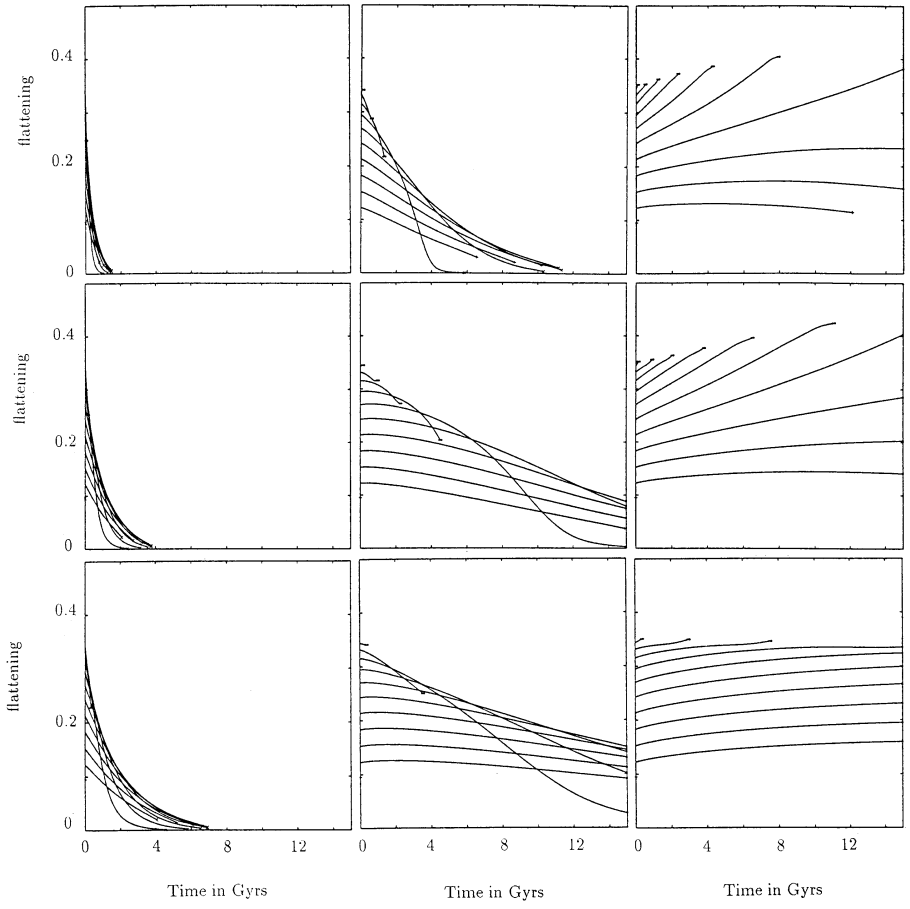

Fig. 3. Evolution of half-mass flattening as a function of time in Gyrs, for clusters with 15% of rotation energy and α = 3.5 initially. Columns correspond to initial masses of 10^4, 10^5 and 10^6 $M_\odot$ from left to right. Rows correspond to Galactocentric distances of 3, 8 and 14 kpcs from top to bottom. The various tracks correspond to initial values of W_0 ranging from 2 to 7 from top to bottom in each diagram (see Sect. 3.1 for details).

clusters are either dissolved or collapsed. This tendency is also apparent on Fig. 2 which shows that mass loss is less efficient for the more distant clusters; mass loss is also quite naturally more efficient on the less concentrated clusters. Reversely, the timescale for stellar evolution is independent of the Galactocentric distance. We note that, due to our differing treatments of two-body relaxation and stellar evolution, we find a smaller tendency to dissolve clusters than in Chernoff and Shapiro (1987), although the general trends are quite similar. Incidentally, these differences give some iindications of the theoretical uncertainties associated with this type of simplified dynamical modelling.

The most stricking new feature seen on the lower half diagrams of Fig. 1 is the increased tendency of all cluster models to dissolve as a result of rotation. The lower limit in initial concentration W_0 for survival has typically increased by $\Delta W_0 \sim 1$. This obtains for the following reason. As soon as the rotation energy of the cluster $T_{\rm rot.}/T_t$ exceeds $\sim 5\%$, the evolution of the concentration due to internal relaxation uncouples from the mass loss (in this regard, rotating King models differ from nonrotating ones). In particular, the evolution tends to occur along lines of constant concentration, until the rotational energy has decreased enough (see paper II). In the meantime, the tendency to dissolution induced by stellar evolution and gravitational shocking is not counteracted by internal relaxation. We note that the magnitude of this effect is underestimated in our model. Indeed, rotating King models have an extra support against gravity, with respect to nonrotating ones, which tends to shift the mass distribution of the model outwards, and consequently the efficiency of gravitational shocking should be larger for rotating models than for nonrotating ones, a feature which is ignored in our modelling.

It has often been pointed out in the past that clusters seem to be more highly concentrated than implied by evolutionary considerations alone. However, some caution is called for. Indeed, the effects of both stellar evolution and gravitational shocking on cluster dissolution are underestimated in our calculations. Also, it is significant that these two processes as well as rotation tend to make globular clusters dissolve. It is still possible that a precise modelling of the known processes would be sufficient to explain the high concentrations seen in globular clusters today.

The evolution of the cluster flattening (measured at the cluster half-mass) is represented on Fig. 3 for an initial rotation energy of 15%. Diagrams in a column correspond to cluster masses of 10^4, 10^5 and 10^6 $M_\odot$, from left to right, whereas diagrams in a row correspond to galactocentric distances of 3, 8, and 14 kpcs from top to bottom. Note that the cluster flattening decreases with increasing W_0 at t = 0. Fig. 3 shows clearly that relaxation dominates in the less massive clusters (10^4 $M_\odot$), whose initial flattening is almost completely erased in a fraction of a Hubble time. Reversely, stellar evolution and tidal shocking induce a significant increase of the flattening of the most mas-

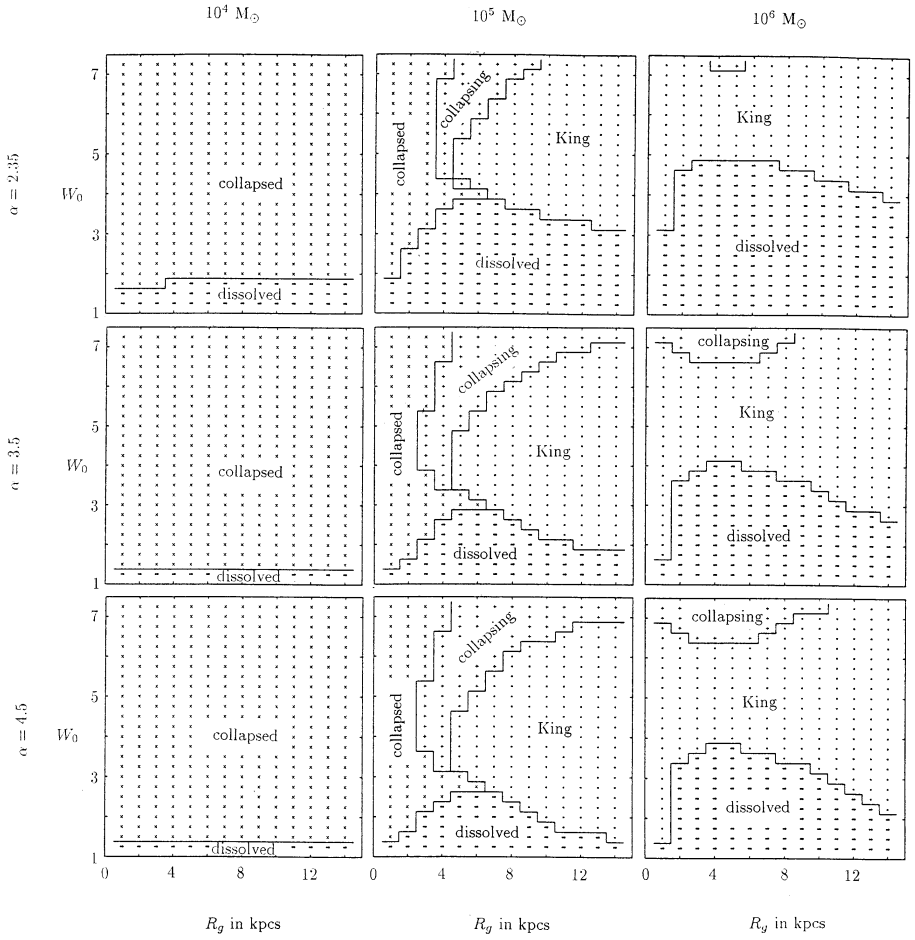

Fig. 4. Endstates of non rotating globular clusters after 1.5×10^{10} Gyrs of evolution (see Sect. 3.2). Columns correspond to initial cluster masses of 10^4, 10^5 and 10^6 M$_\odot$ from left to right. Lines to α = 2.35, 3.5 and 4.5 from top to bottom. In each diagram the horizontal axis gives the Galactocentric position of the cluster, while the vertical axis represents its initial concentration W_0. The four possible outcomes quoted on the diagrams correspond to cluster models which are either collapsed, collapsing, dissolved, or still on the King sequence.

sive clusters, although it is most dramatic in those which finally dissolve due to gravitational shocking. These diagrams show clearly that evolutionary effects can produce a mass/flattening or equivalently luminosity/flattening correlation. Such a correlation would already follow by internal relaxation alone, as the relaxation timescale increases with mass, but it is amplified by gravitational shocking and stellar evolution. A similar correlation has already been reported in the literature (Van den Bergh, 1983), and it is tempting to attribute it to evolutionary effects. The key role played by internal relaxation on the evolution of globular cluster flattening that we just pointed out is also directly apparent in the flattening/half-mass relaxation time correlation established by Davoust and Prugniel (1990) for the Galactic globular clusters.

We finally note that the dynamical correlation presented here is less strong at larger Galactocentric distances, as relaxation becomes less efficient. However, this effect is weaker; indeed, we searched for a flattening/Galactocentric distance in the available data, and found none. More generally, we note that both rotating and nonrotating clusters more massive than 10^5 M$_\odot$ appear to be little affected by evolutionary effects, if they do not orbit within the first eight (or so) inner kiloparsecs of the Galaxy.

The angular momentum (not displayed on figures here) is always a decreasing function of time, as all three modelled processes result in a loss of angular momentum. Except for the less massive clusters, the largest loss is exhibited by the clusters which head fastest towards dissolution. Clusters less massive than 10^5 M$_\odot$ which have survived dissolution have lost at least 50% of their initial angular momentum. On the contrary, massive clusters lose little angular angular momentum (typically of the order of 20%). Generally speaking, this implies that the angular momentum of the clusters seen today is within a factor of two or three a measure of their initial angular momentum. This may possibly, although indirectly, constrain the globular cluster formation scenarios.

3.2. Survey

The effects just discussed can be more globally apprehended on Figs. 4 and 5, which display the state of globular clusters at the end of our computations. Initially nonrotating clusters are shown on Fig. 4, while Fig. 5 presents clusters with a initial rotational energy equal to 15%. Similar diagrams have also been produced for different values of the rotation energy, but again, the results can be extrapolated from the diagrams presented here. Each figure contains nine diagrams. Diagrams on a same column pertain to clusters having the same mass, 10^4, 10^5 and 10^6 M$_\odot$ from left to right respectively. Diagrams on a same row differ by the mass spectrum index α, which takes values equal to 2.35 (Salpeter initial mass function), 3.5 and 4.5 from

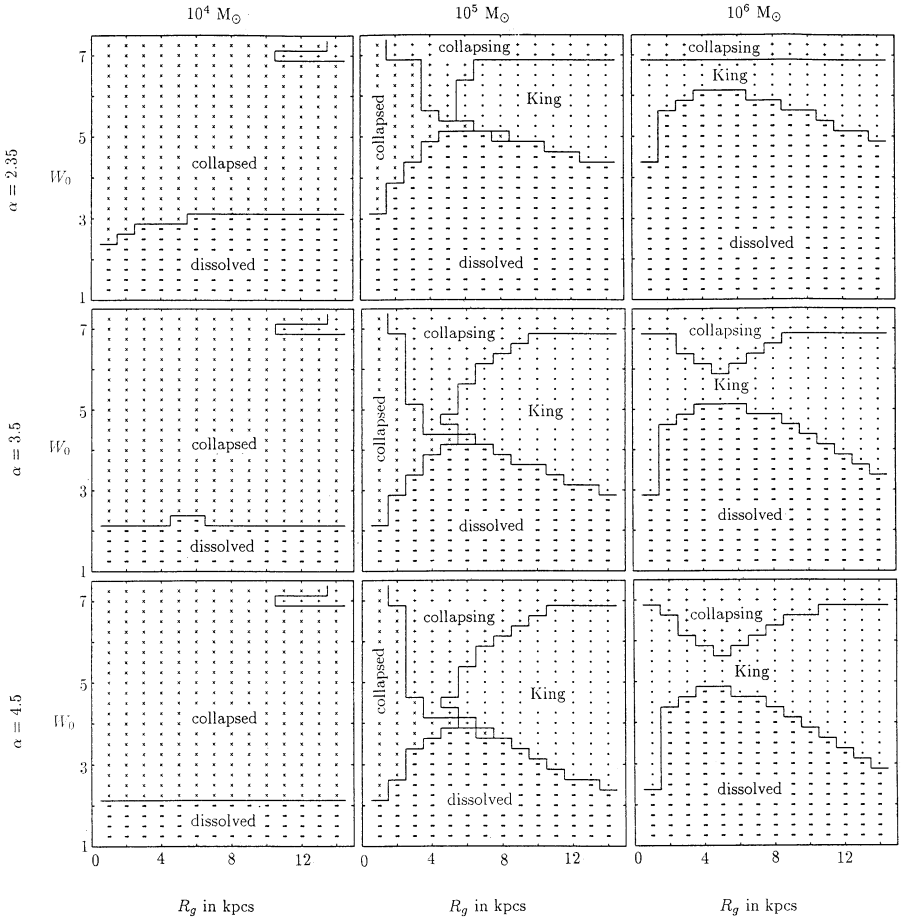

Fig. 5. Same as Fig. 4, but for 15% of initial rotation energy

top to bottom. These values were chosen for ease of comparison with the survey conducted by Chernoff and Shapiro (1987) for nonrotating clusters. On each diagram, the horizontal axis gives the galactocentric distance of a cluster model, while the vertical axis gives its initial concentration parameter W_0. Therefore each point in each diagram represents a unique cluster model, whose endstate after a Hubble time of evolution is specified by the evolutionary model of Sect. 2. Each diagram is thus divided into four regions at most, corresponding to the four possible outcomes of the evolution (cluster collapsed, collapsing, dissolved, or still on the King sequence). Remember that clusters with $W_0 < 1.5$ are assumed to dissolve, so that the dissolution region limit in the two lower left diagrams fo Fig. 4 is rather arbitrary.

As in the previous subsection, we first briefly discuss the diagrams for nonrotating clusters. These diagrams clearly show that the initial cluster mass plays a dominant role in its evolution, due to the dependence of the internal half-mass relaxation time-scale on the cluster mass. Most "light" clusters (the leftmost column) are collapsed; the other dissolved, due to their weak initial binding. Moving rightward from one column to the next, the relaxation time-scale increases, implying a higher relative efficiency of gravitational shocking and stellar evolution with respect to internal relaxation and a correlative increased efficiency of dissolution; the shape of the dissolution limit is explained by the variation of efficiency of internal relaxation and gravitational shocking with Galactocentric distance. Furthermore, not all clusters which do not dissolve have time to collapse when the relaxation time-scale increases, especially at large distances, which explains the appearance and increasing size of regions in the diagrams corresponding to clusters still belonging to the King sequence when one moves from one column to the next. Finally, moving downwards from one row to the next results in a decreas of efficiency of stellar evolution, whose effect is mainly to shift downwards in the diagrams the borders of the various regions. These diagrams also show that our evolutionary model produces a smaller number of dissolved clusters than in Chernoff and Shapiro (1987).

Comparing Figs. 4 and 5, the most obvious change concerns the border of the dissolution region. Clusters need an increase in initial concentration $\Delta W_0 \sim 1$ to survive, as already pointed out in our discussion of the evolutionary tracks. We also note from the evolutionary tracks that the rotating 10^4 M$_\odot$ clusters which do not dissolve loose a significantly larger proportion of their mass than the nonrotating ones, sometimes up to 90% of their mass. One can wonder whether these clusters do not in fact entirely dissolve, as some of the assumptions underlying our modelling are invalidated for clusters containing such a small number of stars at the end of the computation. The second most obvious change concerns a noticeable increase of

the number of collapsing clusters, at high initial concentrations. This reflects mostly the smaller concentrations required in rotating clusters for the onset of the gravothermal catastrophe (see paper I), through the varying efficiency of the three modelled processes on the decrease of the relative rotational energy.

4. Discussion

Let us first briefly summarize the main features and results of this investigation. First, internal relaxation produces a systematic decrease of the cluster concentration and flattening; however, the concentration tends to remain nearly constant until the relative rotational energy of the cluster becomes $\lesssim 5\%$. Gravitational shocking produces an increase of concentration if $W_0 \gtrsim 4$ and a decrease otherwise. Stellar evolution always results in a decrease of the cluster concentration. Both processes induce an increase of the cluster flattening. For very massive clusters, internal relaxation is not very efficient, and the cluster flattening tends to increase due to gravitational shocking and stellar evolution. On the other hand, the flattening of the less massive clusters decreases quite sensibly in the evolution. As the cluster mass is directly correlated to its half-mass relaxation timescale on one hand, and to its luminosity on the other, this strongly suggests that the relaxation time/flattening correlation (Davoust and Prugniel 1990) and luminosity/flattening correlation (Van den Bergh and Morbey 1984) are linked to the cluster evolution rather than to clusters initial conditions.

The flattening of the Magellanic Clouds clusters is significantly larger than for the Galactic ones (Frenk and Fall 1982). These clusters are in fact widely spread in age, and Frenk and Fall (1982) have shown that their flattening correlates with their age. We have investigated this problem by conducting an evolutionary survey of the Large Magellanic Cloud clusters similar to the one presented in the paper for the Galactic ones. We found that the spread in age can indeed produce significant differences in cluster flattening (assuming initial conditions independent of the cluster age, i.e. of its time of formation). Furthermore, the Large Magellanic Cloud differs from the Galaxy in two respects: its mass is smaller, and it has no disk[1]; consequently, internal relaxation is much less efficient so that globular cluster flattening evolves about twice less fast there than here, in spite of the absence of gravitational shocking. However, this effect seems weaker than the spread in age on the evolution of the cluster flattening. More detailed results on the Large Magellanic Cloud clusters (as well as for the Galactic clusters) can be found in Lagoute (1995), and will be provided on request.

At last, but not least, rotation produces two major differences on the evolution of globular clusters. First, the lower limit in initial concentration needed for globular clusters to survive dissolution must be larger by $\Delta W_0 \sim 1$ for rotating clusters than for their nonrotating counterparts. This result is largely independent of any other cluster parameter. Second, core collapse begins at lower concentrations. We also note that generally speaking the total angular momentum of most clusters changes by less than a factor of two or so during the evolution, implying that clusters are formed with $\lambda \sim 0.1$ within a factor of two, and with qualifications connected to the neglect of radial velocity dispersion anisotropy (see below).

Rotation, gravitational shocking and stellar evolution all reduce the domain of survival of globular clusters to higher concentrations, so that one is tempted to believe that the high concentrations observed in globular clusters today is a consequence of globular cluster evolution. However, quite a number of serious shortcomings of the present study must be overcome before one could distinguish evolutionary effects from spread in initial conditions, and assert or disprove such a conjecture.

Multi-mass cluster models are needed, as the inclusion of a spectrum of mass is known to significantly shorten the timescale of internal evolution, while changing the efficiency of stellar evolution; Chernoff and Weinberg (1990) concluded that the overall effect is to delay the onset of core collapse, but a detailed study in presence of rotation and gravitational shocking is called for.

Our simplified evolutionary model cannot follow clusters through and beyond core collapse. Also, as we consider distributions function which depend on two integrals of the motion only, we have ignored the radial anisotropy of the velocity dispersion. Both defects are serious, and connected to one another. Indeed, a significant number of clusters appear to be concentrated enough to undergo core collapse. Furthermore, a sizeable fraction of these clusters are flattened in such a way that their corresponding rotating King model should be dynamically unstable, at least according to the criterion of Ostriker and Peebles (1974). This issue can be significantly alleviated if radially anisotropic models are used instead, as these would allow a fast enough rotation of the core to produce the observed flattening, while corresponding to a lower total rotation energy, due to the steeper density profile in the halo.

We have ignored the possibility that cluster flattening is connected to the anisotropy of the velocity ellipsoid, rather than to rotation, as in elliptic galaxies. Such an anisotropy would also decrease by internal relaxation, and possibly yield similar observational signatures. However, one would expect that the flattening induced by velocity anisotropy would decrease faster, at least in the cluster central regions, than the flattening produced by rotation, as the first one decreases on the internal relaxation timescale, while the second one is related to the evaporation timescale. In his PhD thesis, Goodman (1983) has studied a few models flattened by velocity anisotropy and found that their flattening indeed decreased faster than the flattening of rotating models, but with only a modest difference in evolution rates. It is difficult to compare his rotating models with ours, but we found indications that his models seem to contain in fact a large rotation energy, which can significantly speed up both the evaporation timescale and the evolution rate of their flattening, and might explain his somewhat surprising result. In any case, the issue of velocity anisotropy should be more carefully investigated before more definite conclusions can be drawn.

We have ignored the direct effect of the Galactic tide on the evolution of the angular momentum of globular clusters. A

[1] However, it has a strong bar.

simple order of magnitude estimate of the static tide ("planet-satellite" type of tidal interaction) was inconclusive, because we were unable to estimate with enough precision the equivalent Love number of globular clusters; the static tide can be either negligible or dominant. Also, it is known from the study of binary star tides that the dynamic tide can in some circumstances be significantly more efficient than the static one. In stars, the dynamic tide results from the excitation of waves by the tidal potential. In a gaseous model of globular clusters, an order of magnitude calculation shows that the wavelength of these waves is smaller than the typical interstellar distances, and therefore cannot be excited and propagate, except in the cluster core, which is nearly isothermal, so that this wavelength tends to become infinite, and the waves to couple efficiently to the tidal potential. If effective, this process might affect the angular momentum of the cluster core, and, possibly of the whole cluster through any type of coupling of the core to the rest of the structure. In any case, a more quantitative study is required to assess whether Galactic tides play any role in the evolution of the angular momentum and flattening of globular clusters.

Acknowledgements. We thank Jeremy Goodman for providing us with his unpublished work on the rotation of globular clusters.

Appendix A: evolution rates induced by two-body encounters

First, we define, after King (1966), a reduced potential energy W, a reduced kinetic energy η, and we also introduce a reduced azimuthal velocity α, defined by

$$W = -\beta(\Phi - \Phi_t)\,, \tag{A1}$$

$$\eta = \frac{\beta v^2}{2}\,, \tag{A2}$$

$$\alpha = \Omega(2\beta)^{1/2} r \sin\theta\,, \tag{A3}$$

where v is the stellar velocity, (r, θ, φ) the star position in spherical coordinates, and Φ the self-gravitation potential, computed self-consistently from Poisson's equation. Due to the assumed axisymmetry, quantities in the cluster are independent of φ.

With these definitions, the mass density ρ in the cluster is given by

$$\rho = \frac{4\pi C m}{3(\beta/2)^{3/2}} \exp(W) Q(W,\alpha)\,, \tag{A4}$$

with

$$Q(W,\alpha) = \int_0^W d\eta\ \exp(-\eta) h(\eta,\alpha)\,, \tag{A5}$$

$$h(\eta,\alpha) = \frac{3}{\alpha^3}\left[\alpha\eta^{1/2}\cosh\left(\alpha\eta^{1/2}\right) - \sinh\left(\alpha\eta^{1/2}\right)\right]\,. \tag{A6}$$

The mass density in the cluster center ρ_0 reads

$$\rho_0 = \frac{4\pi C m}{3(\beta/2)^{3/2}} \exp(W_0) Q_0(W_0)\,, \tag{A7}$$

where

$$Q_0(W_0) \equiv \int_0^{W_0} d\eta\ \exp(-\eta)\eta^{3/2}. \tag{A8}$$

It is also useful to introduce the King core radius r_c,

$$r_c = \left(\frac{9}{4\pi G\rho_0\beta}\right)^{1/2}, \tag{A9}$$

and a reduced radial coordinate $\xi \equiv r/r_c$.

The local mean azimuthal velocity $\langle v_\phi\rangle$ and the mean quadratic velocity $\langle v^2\rangle$ read

$$\langle v_\phi\rangle = \frac{1}{\alpha}\left(\frac{2}{\beta}\right)^{1/2} - \frac{3}{(2\beta)^{1/2}}\frac{1}{Q(W,\alpha)} \times \int_0^W \exp(-\eta)\left[\frac{2}{\alpha^2}\eta\sinh\alpha\eta^{1/2} - \frac{4}{3\alpha}h(\eta,\alpha)\right] d\eta, \tag{A10}$$

$$\langle v^2\rangle = \frac{3}{\beta Q(W,\alpha)}\int_0^W \exp(-\eta)\left[\frac{4}{\alpha^2}h(\eta,\alpha) + \frac{2\eta}{\alpha^3}\left(\alpha\eta^{1/2}\cosh\left(\alpha\eta^{1/2}\right) - 3\sinh\left(\alpha\eta^{1/2}\right)\right)\right] d\eta. \tag{A11}$$

Introducing $\tilde\rho = \rho/\rho_0$, $\tilde j^2 = 3/2(\langle v^2\rangle - \langle v_\varphi\rangle^2)$, $x = \tilde j v_e$ (where $v_e = [2(\Phi_t - \Phi)]^{1/2}$ is the local escape velocity) and $y = \tilde j\langle v_\varphi\rangle$, the loss rates we are interested in read

$$\left(\frac{dM_t}{dt}\right)_{\rm rel.} = -\frac{1}{T_0}\frac{6\exp(-W_0)}{Q(W_0)}\rho_0 r_c^3 \times \int d\xi \int d\theta\tilde\rho\sin\theta\xi^2\exp[\gamma(x^2+y^2)]H(x,y), \tag{A12}$$

$$\left(\frac{dE_t}{dt}\right)_{\rm rel.} = \Phi_t\frac{dM}{dt}, \tag{A13}$$

$$\left(\frac{dL_t}{dt}\right)_{\rm rel.} = -\frac{1}{T_0}\frac{6\exp(-W_0)}{Q(W_0)}\rho_0\left(\frac{2}{\beta}\right)^{1/2} r_c^4 \times \int d\xi \int d\theta\tilde\rho\sin^2\theta\xi^3\exp[\gamma(x^2+y^2)]H'(x,y)\,, \tag{A14}$$

where T_0 is the central relaxation time,

$$T_0^{-1} = 2\pi G^2 m^2 {\rm Ln}\Lambda\left(\frac{\beta}{2}\right)^{1/2} n_0, \tag{A15}$$

and where the other quantities are defined by

$$\gamma = \frac{j}{\tilde j}\frac{l\xi\sin\theta}{2y}, \tag{A16}$$

$$H(x,y) = \left(\frac{j}{\tilde j}\right)^2\sum_{i=1}^6 P_i(x,y)I_i(x,y,\gamma), \tag{A17}$$

$$H'(x,y) = y\left(\frac{(\beta/2)^{1/2}}{\tilde j}\right)^3\sum_{i=1}^6 P_i'(x,y)I_i(x,y,\gamma), \tag{A18}$$

$$P_1 = \left(\frac{x^2-y^2}{2}\right)^2, \tag{A19}$$

$$P_2 = \left(\frac{x^2-y^2}{2}\right), \tag{A20}$$

$$P_3 = \frac{1}{4}, \tag{A21}$$

$$P_4 = 0, \tag{A22}$$

$$P_5 = x^2, \tag{A23}$$

$$P_6 = 0, \tag{A24}$$

$$P'_1 = \left(\frac{x^2-y^2}{2}\right)^2 \left(\frac{x^2+y^2}{2y^2}\right), \tag{A25}$$

$$P'_2 = \left(\frac{x^2-y^2}{2}\right) \left(\frac{x^2+3y^2}{4y^2}\right), \tag{A26}$$

$$P'_3 = \frac{x^2+3y^2}{4y^2}, \tag{A27}$$

$$P'_4 = -\frac{1}{2y^2}, \tag{A28}$$

$$P'_5 = x^2 \left(\frac{x^2+y^2}{2y^2}\right), \tag{A29}$$

$$P'_6 = -\frac{x^2}{2y^2}, \tag{A30}$$

$$I_1 = \frac{1}{y}\int_{x-y}^{x+y} \frac{1}{X_e} \exp(-\gamma X_e^2) s(X_e)\, dX_e, \tag{A31}$$

$$I_2 = \frac{1}{y}\int_{x-y}^{x+y} X_e \exp(-\gamma X_e^2) s(X_e)\, dX_e, \tag{A32}$$

$$I_3 = \frac{1}{y}\int_{x-y}^{x+y} X_e^3 \exp(-\gamma X_e^2) s(X_e)\, dX_e, \tag{A33}$$

$$I_4 = \frac{1}{y}\int_{x-y}^{x+y} X_e^5 \exp(-\gamma X_e^2) s(X_e)\, dX_e, \tag{A34}$$

$$I_5 = \frac{1}{y}\int_{x-y}^{x+y} X_e \exp(-\gamma X_e^2) t(X_e)\, dX_e, \tag{A35}$$

$$I_6 = \frac{1}{y}\int_{x-y}^{x+y} X_e^3 \exp(-\gamma X_e^2) t(X_e)\, dX_e, \tag{A36}$$

$$s = \pi \mathrm{erf}(X_e)\left[-\frac{1}{X_e}+\frac{1}{2X_e^3}\right] - \pi^{1/2}\exp(-X_e^2)\left[\frac{3}{X_e^2}\right], \tag{A37}$$

$$t = \pi \mathrm{erf}(X_e)\left[\frac{1}{X_e}-\frac{1}{2X_e^3}\right] + \pi^{1/2}\exp(-X_e^2)\left[\frac{1}{X_e^2}\right]. \tag{A38}$$

(A39)

The various functions of one and two variables involved in these expressions have been tabulated to save computational time, as well as the properly adimensionalized loss terms. In the computations reported here, we have adopted $m = 0.7\ \mathrm{M}_\odot$ for definiteness in the two-body relaxation time [Eq. (A15)], but using a varying mean mass would not change much the results, in regard of the modelling uncertainties of our approach.

References

Agekian, T.A., 1958, Soviet Astron.–AJ, 2, 22

Ambartsumian, V.A., 1938, Scient. Trans. Leningrad Univ., 20, 19. Translated in english in *Dynamics of Star Clusters*, IAU Symposium No 113, 1985, J. Goodman and P. Hut, Eds., p 521

Bahcall, J.N., Schmidt, M., Soneira, R.M., 1982, ApJLet., 258, L23

Chernoff, D.F., Kochanek, C.S., Shapiro, S.L., 1986, ApJ, 309, 183

Chernoff, D.F., Shapiro, S.L., 1987, ApJ, 322, 113

Chernoff, D.F., Weinberg, M.D., 1990, ApJ, 351, 121

Cohn, H., 1980, ApJ, 242, 765

Davoust, E., 1986, A&A, 166, 177

Davoust, E., Prugniel, P., 1990, A&A, 230, 67

Frenk, C.S., Fall, S.M., 1982, MNRAS, 199, 565

Goodman, J., 1983, PhD thesis, Princeton (unpublished)

Geyer, E.H., Hopp, U., Nelles, B., 1983, A&A, 125, 359

Gebhardt, K., Fischer, P., 1995, AJ, 109, 209

Inagaki, S., 1985, in *Dynamics of Star Clusters*, IAU Symposium No 113, J. Goodman and P. Hut, Eds., p 189

Katz, J., 1980, MNRAS, 190, 497

King, I., 1966, AJ, 71, 64

Lagoute, C., Longaretti, P.-Y., 1996, A&A, 308, 441 (paper I)

Lagoute, C., 1995. PhD thesis, Toulouse (unpublished)

Longaretti, P.-Y., Lagoute, C., 1996, A&A, 308, 453 (paper II)

Lupton, R., Gunn, J.E., Griffin, R.F., 1987, AJ, 93, 1114

Miller, G.E., Scalo, J.M., 1979, ApJ Sup., 41, 513

Ostriker, J.P., Spitzer, L., Chevalier, R.A., 1972, Apj Lett., 176, L51

Ostriker, J.P., Peebles, P.J.E., 1973, ApJ, 186, 467

Piotto, G., 1995, in *Dynamical Evolution of Star Clusters – Confrontation of Theory and Observations*, IAU Symposium No 174, J. Makino and P. Hut, Eds. (to be published)

Shapiro, S.L., Marchant, A.B., 1976, ApJ, 210, 757

Spitzer, L., 1940, MNRAS, 100, 396

Spitzer, L., Chevalier, R.A., 1973, ApJ, 183, 565

Taillet, R., Salati, P., Longaretti, P.-Y., 1996, ApJ, 461, 104

Van den Bergh, S., 1983, PASP, 95, 839

Van den Bergh, S., Morbey, C.L., 1984, 283, 598

Weinberg, M.D., 1994a, AJ, 108, 1398

Weinberg, M.D., 1994b, AJ, 108, 1403

Weinberg, M.D., 1994a, AJ, 108, 1414

White, R.E., Shawl, S.J., 1987, ApJ, 317, 246

Wiyanto, P., Kato, S., Inagaki, S., 1985, PASJ, 37, 715

This article was processed by the author using Springer-Verlag LaTeX A&A style file *L-AA* version 3.